

Nonlinear optical processes in two and multilevel atoms: a theoretical and numerical study

M Patel¹, G De Jager², Z Nkosi³ and K Govender⁴

^{1,3,4} Department of Electrical, Electronic and Computer Engineering, Cape Peninsula University of Technology, Symphony Way, Bellville, Cape Town, 7535, RSA

² Department of Electrical Engineering, University of Cape Town, Rondebosch, 7701, RSA

E-mail: ¹210230177@mycput.ac.za, ²Gerhard.DeJager@uct.ac.za, ³NkosiZ@cput.ac.za,

⁴GovenderK@cput.ac.za

Abstract. In this paper we report on the study of two-level and multilevel atoms interacting with one or more laser beams. The system is analyzed using the semi-classical approach where the dynamics of the atom is described quantum mechanically using Liouville's equation, while the laser is treated classically using Maxwell's equations. Firstly, we present results of a two-level atom interacting with a single laser beam and demonstrate Rabi oscillations between the two levels. We then examine the effects of laser modulation on the dynamics of the atom. The behaviour of the laser as it propagates through the atomic ensemble is studied by solving Maxwell's equations numerically. We study the nonlinear process called four-wave mixing that occurs when two or more pump beams, having different frequencies, interact with four different levels of a nonlinear medium. We make use of general energy levels in a diamond configuration. We present results of four-wave mixing for various detuning.

1. Introduction

Recently there has been a number of papers describing entangled photon pair generation using four-wave mixing in Rubidium atomic ensemble[1, 2, 3]. At the Cape Peninsula University of Technology an experiment is under development to investigate the properties of entangled photons generated by four-wave mixing in warm and cold Rubidium atoms. These atoms will be used for quantum key distribution in the future. In this paper we report on computational simulations of this process.

We report on the computational study of the interaction between laser beams and two and multilevel atoms. We use a semi-classical approach in which the dynamics of the atoms (described by the density matrix elements) are governed by the Von Neumann-Liouville equation,

$$i\hbar \frac{\partial \rho}{\partial t} = [\hat{H}, \hat{\rho}] + \text{relaxation terms} \quad (1)$$

while the laser beam is described by the wave equation derived from Maxwell's equations. The Hamiltonian of the total system is $\hat{H} = \hat{H}_0 + \hat{H}_I$, where \hat{H}_0 is the unperturbed Hamiltonian and \hat{H}_I is the interaction term. The relaxation terms contain the dissipative effects. We first discuss a two level atom interacting with a single laser beam and examine the dynamics of the populations and coherence terms of the density matrix elements. Thereafter we examine the behaviour of the laser beams as it propagates in multilevel atoms.

The overview of the paper is as follows: Section 2 describes the interaction of a two level atom with a single laser beam. Results showing the effects of a uniform and modulated laser beam are given. The study of the two-level atom is included to introduce basic ideas such as Rabi frequency, detuning and density matrix elements. Four-wave mixing is discussed in Section 3. Results are given for various parameters.

2. Laser-atom interactions

The interaction between a laser beam and a sample of stationary atoms having only two possible energy levels (separated in frequency by ω_0) has the following interaction Hamiltonian:

$$\hat{H}_I = -e\vec{E} \cdot \hat{\vec{D}} \cos \omega t \quad (2)$$

Here $-e\hat{\vec{D}}$ represents the dipole moment operator of the atom, \vec{E} is the electric field or amplitude of the laser beam and $\cos \omega t$ represents the time variation of the electric field of the laser beam where ω is the laser radian frequency. \hat{H}_I is then used in the Von Neumann Liouville equation to describe the time evolution of the density matrix elements of the system. The Von Neumann equation is used to derive the following equations for a two level atom (called Optical Bloch equations):

$$\frac{\partial \rho_{11}}{\partial t} = \frac{1}{2}i\Omega(\rho_{12} - \rho_{21}) + 2\gamma_{sp}\rho_{22} \quad (3)$$

$$\frac{\partial \rho_{12}}{\partial t} = \frac{1}{2}i\Omega(\rho_{11} - \rho_{22}) + [i(\omega_0 - \omega) - \gamma_{sp}]\rho_{12} \quad (4)$$

$$\frac{\partial \rho_{21}}{\partial t} = -\frac{1}{2}i\Omega(\rho_{11} - \rho_{22}) + [-i(\omega_0 - \omega) - \gamma_{sp}]\rho_{12} \quad (5)$$

$$\frac{\partial \rho_{22}}{\partial t} = -\frac{1}{2}i\Omega(\rho_{12} - \rho_{21}) - 2\gamma_{sp}\rho_{22} \quad (6)$$

where $\Omega = eE\langle D \rangle / \hbar$ is called the Rabi frequency and γ_{sp} represents a decay/de-coherence coefficient. ρ_{11} and ρ_{22} tells us the probability of the atom being in the ground and excited states, respectively. ρ_{12} and ρ_{21} are the interference terms of the atom indicative of superposition. We solve the above numerically.

2.1. Results

Results of the numerical solution of Equations 3-6 are given in Figures 1-2. Figure 1 corresponds to a uniform laser beam and Figure 2 deals with a modulated laser beam. In Figure 1, the blue curve represents ρ_{11} , the red curve ρ_{22} , the green curve ρ_{12} and the magenta curve ρ_{21} . The laser is switched on at $t = 0$ s with $\rho_{11} = 100\%$ and $\rho_{22} = 0\%$. Rabi oscillations are demonstrated in Figure 1A where $\omega_0 - \omega = 0$. In Figure 1B the laser is detuned i.e. $\omega_0 - \omega \neq 0$. The interference between Ψ_1 and Ψ_2 is decreased, where Ψ_i is the wave function corresponding to level i . A small dissipation is introduced in Figure 1C in the form of γ_{sp} . This results in the interference between Ψ_1 and Ψ_2 to decay to the point where the probability of superposition is close to 0%. The phase space plots in Figure 1D are related to Figures 1A-C: Rabi oscillation where the atom continues on the same path infinitely, (— black); laser detuning where the atom continues on the same path but at a different frequency to the Rabi frequency, (— purple); dissipation where the atom never follows the exact same path and diminishes at 0, (— orange).

The laser frequency, ω in the above equations, equations (3) to (6), is altered by including terms of modulation by means of a sinusoidal variation to the laser frequency. The modulated detuning is then

$$(\omega_0 - \omega) = \delta + D \sin(2\pi f_m t) \quad (7)$$

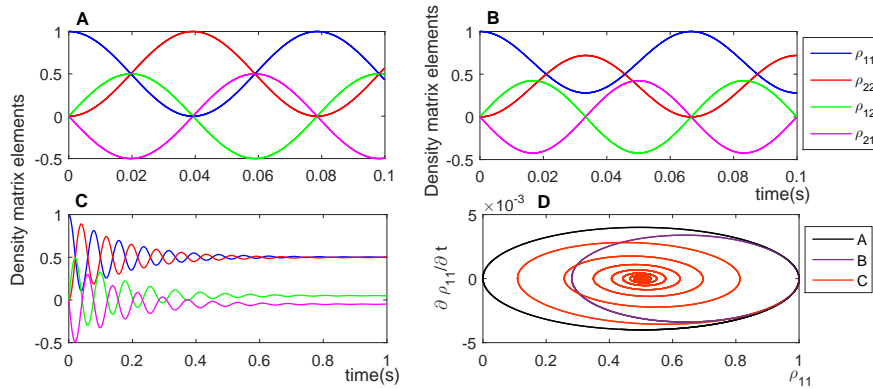


Figure 1. General features of a two-level atom interacting with a uniform laser beam. Plots A-C are the density matrix elements corresponding to (A) zero laser detuning demonstrating Rabi oscillation, (B) non-zero laser detuning, (C) zero detuning with added dissipation. Plot (D) shows the phase space plot, $\partial \rho_{11} / \partial t$ vs ρ_{11} for the above cases.

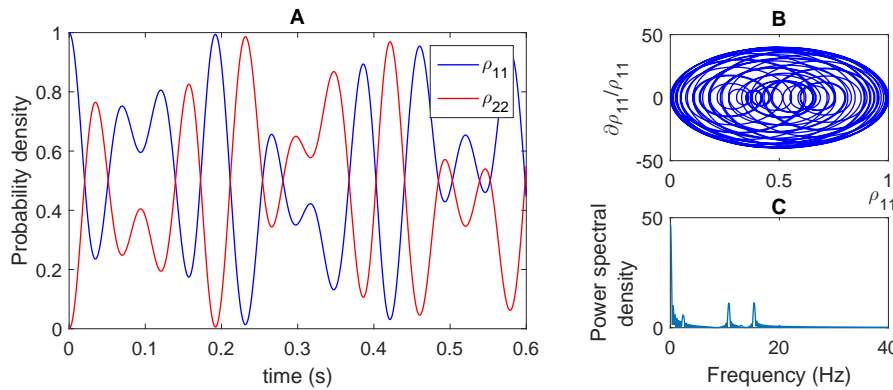


Figure 2. Two-level atom interacting with a laser beam where the modulated frequency is approximately equal to the Rabi frequency and the amplitude of modulation is small. The plots are: (A) time series; (B) phase space plot and (C) fast Fourier transform.

where δ has a fixed value, f_m is the modulation frequency and D represents the level of modulation. Making use of various parameters in equation (7) gives rise to interesting behaviour of the atomic dynamics. These are seen in Figure 2. The time series, Figure 2(A), shows an irregular curve. The phase space plot (B) shows that the atom deviates from the ground state from cycle to cycle - the path does not repeat itself. The atom behaves in a chaotic manner. In the Fourier spectra (C) there are three components that arise at 2.36 Hz, 10.72 Hz and 15.37 Hz, none of which appear at the Rabi frequency, $\Omega = 12.73$ Hz (ignoring the DC component at 0 Hz). These results show that the atom has tendencies to behave in a chaotic manner. Similar results have been seen by Pisipati et al. [4].

3. Nonlinear mixing in multilevel atoms

Next, we study the parametric process of four-wave mixing by having two pump beams, of different frequencies, interact with four levels of a hypothetical atom. Figure 3 shows the energy level structure where $|1\rangle$, $|2\rangle$, $|3\rangle$ and $|4\rangle$ are four relevant energy levels of the atom with $|1\rangle$ being the ground state and $|2\rangle$, $|3\rangle$ and $|4\rangle$ being excited states.

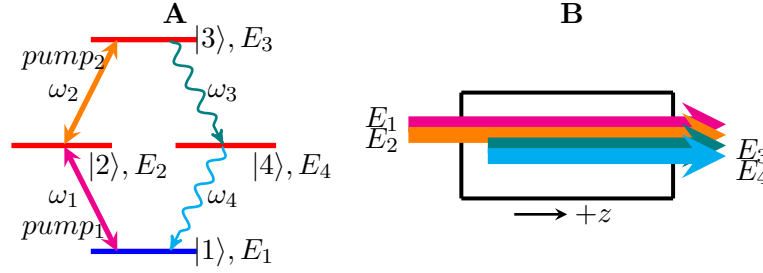


Figure 3. Four-wave mixing geometry. **A-** E_1 to E_4 are the corresponding energies of each level, ω_1 and ω_2 are the frequencies of two pump laser beams and ω_3 and ω_4 are the frequencies of two internally generated photons. **B-** E_1 and E_2 represent the electric fields of the pump beams and E_3 and E_4 represent the internally generated photons (these should not be confused with the energies).

In our analysis co-propagating beams, E_1 and E_2 , having different wavelengths are used as pumps beams. We investigate the production/variation of E_3 and E_4 across the longitudinal section of the sample. We assume that the pump laser beams are strong enough so that they do not get depleted as they propagate through the atomic ensemble. We also assume that all photons propagate in the positive z -direction. The atomic levels are assumed to be such that the photons of frequency ω_1 , ω_2 , ω_3 and ω_4 couple only transitions between $|1\rangle \leftrightarrow |2\rangle$, $|2\rangle \leftrightarrow |3\rangle$, $|3\rangle \leftrightarrow |4\rangle$ and $|4\rangle \leftrightarrow |1\rangle$, respectively, that is, they are very much detuned compared to the other transitions.

We now explain the derivation of the equation needed for predicting the electric fields, E_3 and E_4 . Further details of these derivations are provided in [5]. The behaviour of the electric fields E_3 and E_4 corresponding to frequencies ω_3 and ω_4 respectively are described by Maxwell's equations:

$$\frac{\partial}{\partial z} E_3(z) = i \frac{\omega_3}{2\epsilon c} \frac{N}{V} \mu_{34} \rho_{34}^{(3)} \quad (8)$$

$$\frac{\partial}{\partial z} E_4(z) = i \frac{\omega_4}{2\epsilon c} \frac{N}{V} \mu_{41} \rho_{41}^{(3)} \quad (9)$$

where $\rho_{ij}^{(3)}$ are the third order density matrix elements and are obtained from the master equation. These equations, equations (8) and (9), are derived from Maxwell's wave equation [6] where we have written the polarization in terms of $\rho_{34}^{(3)}$ and $\rho_{41}^{(3)}$.

The total Hamiltonian is

$$H = H_0 + H_I \quad (10)$$

where $H_I = -\hat{\mu} \cdot E$, $-\hat{\mu}$ is the dipole moment of the atom and E is the total electric field. The master equation (Liouville-von Neumann equation) that we solve is

$$\dot{\rho} = -\frac{i}{\hbar} [H'_I, \rho] + \text{relaxation terms} \quad (11)$$

where the interaction Hamiltonian term, H'_I , is in the interaction picture.

Making use of perturbation theory we let

$$\rho = \rho^{(0)} + \lambda \rho^{(1)} + \lambda^2 \rho^{(2)} + \dots \quad (12)$$

and expand and group terms by order to obtain the the population and coherence terms. The third order terms that are important for solving Maxwell's equation for the ω_3 and ω_4 terms are $\tilde{\rho}_{34}^{(3)}$ and $\tilde{\rho}_{41}^{(3)}$. The expansion for $\tilde{\rho}_{34}^{(3)}$ is

$$\begin{aligned} \tilde{\rho}_{34}^{(3)} = \frac{1}{(\Delta_{34} - i\Gamma_{34})} & \left[\frac{1}{\hbar^3} \frac{\mu_{21}\mu_{32}\mu_{14}\tilde{E}_1\tilde{E}_2\tilde{E}_4^*}{(\Delta_{42} + i\Gamma_{42})} \left(\frac{1}{(\Delta_{21} - i\Gamma_{21})} - \frac{1}{(\Delta_{41} + i\Gamma_{41})} \right) \right. \\ & + \frac{1}{\hbar^3} \frac{\mu_{34}|\mu_{14}|^2\tilde{E}_3|\tilde{E}_4|^2}{\gamma_{41}} \left(\frac{2\Gamma_{41}}{\Delta_{41}^2 + \Gamma_{41}^2} \right) - \frac{1}{\hbar^3} \frac{\mu_{21}\mu_{32}\mu_{14}\tilde{E}_1\tilde{E}_2\tilde{E}_4}{(\Delta_{21} - i\Gamma_{21})(\Delta_{31} - i\Gamma_{31})} \\ & \left. - \frac{1}{\hbar^3} \frac{\mu_{34}|\mu_{14}|^2\tilde{E}_3|\tilde{E}_4|^2}{(\Delta_{41} - i\Gamma_{41})(\Delta_{31'} - i\Gamma_{31})} \right] e^{-\omega_3 t} \end{aligned} \quad (13)$$

where Δ_{ij} represents the detuning between levels $|i\rangle$ and $|j\rangle$, Γ_{ij} represents the decay rate of the corresponding coherence ρ_{ij} and γ_{ij} represents the decay of the population ρ_{ii} . μ_{ij} are the matrix elements of the dipole moment μ in the basis $|1\rangle$, $|2\rangle$, $|3\rangle$ and $|4\rangle$. A similar equation is obtained for $\tilde{\rho}_{41}^{(3)}$. Equations for the fourth order terms which give the populations of each state as a function of detuning can be found in [7].

3.1. Results

We solve equations (8) and (9) numerically for various values of z and use updated values of $\tilde{\rho}_{34}^{(3)}$ and $\tilde{\rho}_{41}^{(3)}$ each time. We provide plots of the Rabi frequencies (which are proportional to the electric fields) of the emerging beams. Population values are also provided. Figures 4 and 5 show results of the population as a function of detuning of pump₁ (Δ_{21}) and pump₂ (Δ_{32}).

Figure 4 shows results for pump₁ (Δ_{21}) at a constant negative detuning as pump₂ (Δ_{32}) is varied. The atoms will not get excited from $|1\rangle \rightarrow |2\rangle$ easily due to the negative detuning of pump₁ (Δ_{21}). From the slight decrease in ρ_{11} we can assume that most of the atoms have remained in the ground state. As Δ_{32} decreases, corresponding to a smaller detuning, we see ρ_{22} decreasing slightly. This is because atoms have been excited from $|2\rangle \rightarrow |3\rangle$. At the same time ρ_{33} and ρ_{44} have increased by approximately the same amount. Note that ρ_{33} and ρ_{44} are shifted to the right relative to zero detuning to counteract the negative detuning of pump₁ beam in order to get maximum transfer of population to levels $|3\rangle$ and $|4\rangle$.

Figure 5 shows results for pump₂ (Δ_{32}) at a constant positive detuning as pump₁ (Δ_{21}) is varied. Plots for ρ_{11} and ρ_{22} show a decrease and increase in the populations at the respective levels as Δ_{21} decreases. We see that the plots for ρ_{33} and ρ_{44} have been shifted in the negative direction to counteract the positive detuning of the pump₂ beam in order to get maximum transfer of population to levels $|3\rangle$ and $|4\rangle$.

We note that spontaneously generated photons are directly proportional to the populations ρ_{22} , ρ_{33} and ρ_{44} . There are certain values of detuning for which there is maximum coherent beam intensity while the populations are away from their peak values.

4. Summary and Conclusion

We have investigated laser-atom interactions by first examining a two level atom interacting with a single laser beam where Rabi oscillations have been demonstrated. Dissipation effects show up as decay in the populations and de-coherence terms in the density matrix elements. Chaotic behaviour was also seen to occur when a modulated laser is used.

The analysis was extended to include the nonlinear process called four-wave mixing. One of the advantages of entangled photons generated in cold atoms via four-wave mixing is that they have better spectral characteristics and are better matched for absorption by the same type of atom. Various scenarios have been tested where one laser beam was kept constant while

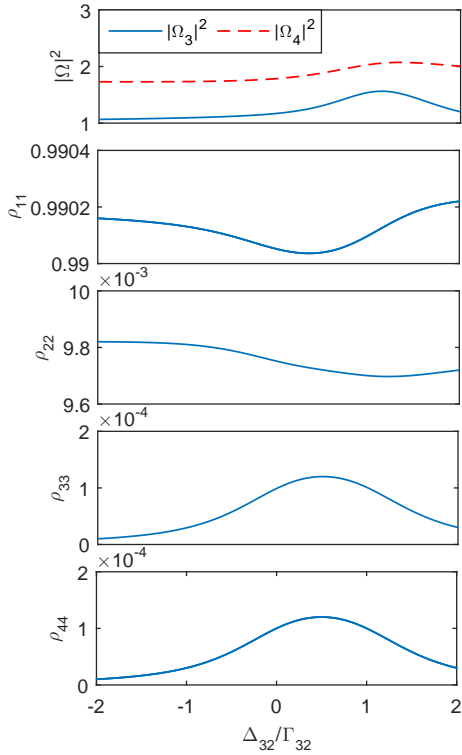


Figure 4. Plots from top to bottom are of Rabi frequency ($|\Omega|^2$) and populations (ρ_{11} , ρ_{22} , ρ_{33} and ρ_{44}) as the pump₂ beam is varied (Δ_{32}/Γ_{32}). Pump₁ beam is kept constant at a negative detuning (Δ_{21}).

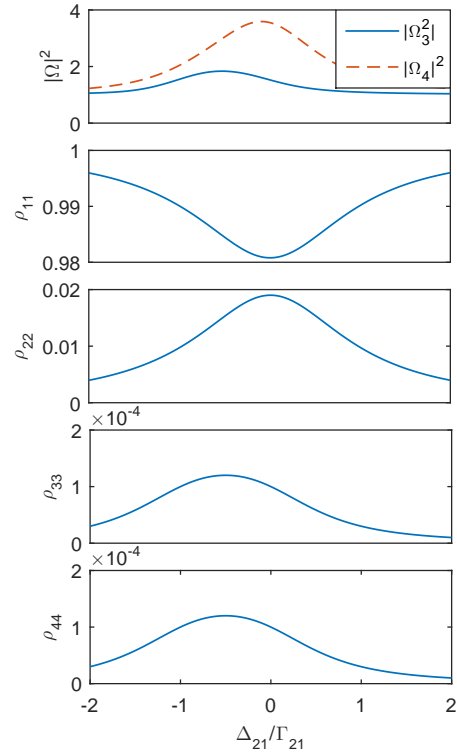


Figure 5. Plots from top to bottom are of Rabi frequency ($|\Omega|^2$) and populations (ρ_{11} , ρ_{22} , ρ_{33} and ρ_{44}) as the pump₁ beam is varied (Δ_{21}/Γ_{21}). Pump₂ beam is kept constant at a positive detuning (Δ_{32}).

the other was varied and vice versa. Maximum intensities of the coherent beams as well as populations were shown to be dependent on the laser detuning.

References

- [1] Srivathsan B, Gulati G K, Brenda C M Y, Maslennikov G, Matsukevich D and Kurtsiefer C 2013 *Phys. Rev. Lett.* **111**(12) 123602
- [2] de Melo N R and Vianna S S 2014 *J. Opt. Soc. Am. B* **31**
- [3] Jen H H and Chen Y C 2016 *Phys. Rev. A* **93**(1) 013811
- [4] Pisipati U, Almakrami I M, Joshi A and Serna J D 2012 *American Journal of Physics* **80**
- [5] Patel M, de Jager G, Wyngaard A and Govender K 2016 *Proc. Int Conf. Comp. Phys*
- [6] Grynberg G, Aspect A, Fabre C and Cohen-Tannoudji C 2010 *Introduction to Quantum Optics: From the Semi-classical Approach to Quantized Light* (Cambridge University Press)
- [7] Patel M 2017 *Numerical study of nonlinear spectroscopy and Four-Wave Mixing in two and multilevel atoms*. Master's thesis (Cape Peninsula University of Technology)